

# Modeling of vapor sorption in glassy polymers using a new dual mode sorption model based on multilayer sorption theory

Haidong Feng\*

*School of Mechanical and Power Engineering, 102, Shanghai Jiao Tong University, 1954 Huashan Road, Shanghai 200030, PR China*

Received 6 January 2006; received in revised form 24 October 2006; accepted 31 October 2006

Available online 5 April 2007

## Abstract

Conventional dual mode sorption (CDMS) model is one of the most effective models in describing vapor sorption isotherms with a concave towards the activity axis in glassy polymers, while engaged species induced clustering (ENSIC) model has been approved to be highly successful in modeling vapor sorption isotherms in polymers with a convex to the activity axis (BET type III) over a wide range. However, neither of them is effective to describe other types of vapor sorption isotherms, especially sigmoidal isotherms. The Guggenheim–Anderson–de Boer (GAB) model fits extremely well with sigmoidal isotherms such as some vapor especially water vapor sorption data in food and related natural materials. However, one assumption of the GAB model for vapor sorption in glassy polymers is inconsistent with the fact that there are two species of sorption sites as the CDMS model assumes. Based on multilayer sorption theory on which the Guggenheim–Anderson–de Boer (GAB) model is based, a new dual mode sorption (DMS) model for vapor sorption in the glassy polymers is deduced. The mathematical meanings and the physicochemical significances of the parameters in the new model are analyzed. The new model has been verified experimentally by some special cases. Comparisons of the new DMS model with the CDMS and the ENSIC models prove that only the new model fits extremely well with all types of vapor sorption isotherms in the glassy polymers.

© 2006 Elsevier Ltd. All rights reserved.

*Keywords:* Glassy polymer; Vapor sorption; GAB model

## 1. Introduction

There are three main types of vapor sorption isotherms in glassy polymers, as shown in Fig. 1(a)–(c), where  $c$  and  $a$  are, respectively, penetrant concentration and activity in the polymers.

Type 1 is concave to activity axis at low activities and almost linear at higher activities [1–3], as shown in Fig. 1(a). Most of the vapor sorption isotherms in glassy polymers are Type 1, such as water vapor sorption isotherms in two polyimide copolymers, PMDA–50DDS/50ODA and BPDA–50DDS/50ODA at 30 °C [2], as illustrated in Fig. 13.

Type 2 regularly referred to as BET type II, is a sigmoidal isotherm, which is concave to the abscissa at low activities and

convex at high activities [4–10], as illustrated in Fig. 1(b). There is an inflection point in the isotherm. Many vapor sorption isotherms in glassy polymers are this type, such as methanol vapor sorption in cellulose acetate [10], as shown in Fig. 16.

Type 3 is always convex to the activity axis [6,10], as shown in Fig. 1(c). Only a few of vapor sorption isotherms in glassy polymers belong to this type, such as ethanol vapor sorption in cellulose acetate [10], as illustrated in Fig. 18.

Two special isotherms, Type 4 and Type 5, both of which are Type 3 actually, should be specially mentioned. Type 4 looks like Type 1, because the downward curvature at relatively high activities is too inconspicuous to be discerned, such as water and ethanol vapor sorption in poly(vinylchloride) (PVC) at 40 °C [11], as shown in Fig. 14. Type 5 looks like Type 3, because the upward curvature at low activities is too inconspicuous to be discerned, such as water vapor sorption in cellulose acetate at 25 °C [10], as displayed in Fig. 17.

\* Tel.: +86 21 62934217; fax: +86 21 64078095.

*E-mail address:* [fhdfhd@sjtu.edu.cn](mailto:fhdfhd@sjtu.edu.cn)

*List of symbols*

$a$	penetrant activity in a polymer
$A$	temperature-dependent constant in GAB model
$A_0$	pre-exponential factor of a temperature-dependent constant in GAB model
$A'$	temperature-dependent constant in new DMS model
$b$	microvoid affinity constant based on pressure
$b_0$	microvoid affinity constant based on activity
$c$	penetrant concentration in a glassy polymer
$c_1$	penetrant concentration in matrix region of a glassy polymer by new DMS model
$c_2$	penetrant concentration in microvoids of a glassy polymer by new DMS model
$c_D$	penetrant concentration in matrix region of a glassy polymer by CDMS model
$c_H$	penetrant concentration in microvoids of a glassy polymer by CDMS model
$C'_H$	Langmuir saturation constant
$C_p$	monolayer sorption capacity
$C_{p1}$	monolayer sorption capacity in matrix region of a polymer
$C_{p2}$	monolayer sorption capacity in microvoid region of a polymer
$C'_p$	weighted mean value of sorption capacity of a polymer to sorbate molecules
$\bar{C}_p$	weighted mean value of polymer sorption capacity to sorbate molecules based on $\bar{s}_1$ and $\bar{s}_2$
$H$	heat given off when a molecule enters sorbed sites of a polymer
$H_L$	heat of condensation of a pure vapor
$H_m$	heat of sorption of monolayer of a vapor
$H_n$	heat of sorption of multimolecular layers of a vapor
$k$	temperature-dependent constant in GAB model
$k'$	temperature-dependent constant in new DMS model
$k_0$	pre-exponential factor of a temperature-dependent constant in GAB model
$k_D$	Henry's law dissolution constant based on pressure
$k_{D0}$	Henry's law dissolution constant based on activity
$k_p$	affinity of a penetrant molecule towards a polymer site
$k_s$	affinity of a penetrant molecule towards a like molecule
$n$	$n$ -layer sorption
$n_p$	polymer segment number
$n_s$	sorbed solvent molecule number
$p$	pressure
$p_0$	vapor saturation pressure
$R$	gas constant
$R^2$	square of the correlation between the response values and the predicted response values
$s$	average number of molecules per sorbed site
$s_1$	average number of molecules per sorbed site in matrix region of a polymer

$s_2$	average number of molecules per sorbed site in microvoid region of a polymer
$\bar{s}_1$	average values of average number of sorbed molecules per site in matrix region of a polymer over the entire range of activity
$\bar{s}_2$	average values of average number of sorbed molecules per site in microvoids of a polymer over the entire range of activity
$T$	temperature
$T_g$	glass transition temperature
$y_i$	experiment value
$\hat{y}_i$	predicted value
$\bar{y}_i$	mean value

*List of abbreviations*

AP	pyromellitic anhydride
BET	Brunauer, Emmet and Teller
BPDA	biphenyl tetracarboxylic dianhydride
CDMS	conventional dual mode sorption
DMS	dual mode sorption
ENSIC	Engaged species induced clustering
GAB	Guggenheim–Anderson–de Boer
MDI	macrodiisocyanate
NTDA– <i>o</i> BAPBDS	a copolymer by copolymerization of 1,4,5,8-naphthalenetetracarboxylic dianhydride (NTDA) and 2,2'-bis(4-aminophenoxy)biphenyl-5,5'-disulfonic acid ( <i>o</i> BAPBDS)
NTDA–BAPBDS	a copolymer by copolymerization of 1,4,5,8-naphthalenetetracarboxylic dianhydride (NTDA) and 4,4'-bis(4-aminophenoxy)biphenyl-3,3'-disulfonic acid
NTDA– <i>o</i> BAPBDS/ <i>m</i> BAPPS(2/1)	a copolymer by copolymerization of 1,4,5,8-naphthalenetetracarboxylic dianhydride (NTDA) and 2,2'-bis(4-aminophenoxy)biphenyl-5,5'-disulfonic acid ( <i>o</i> BAPBDS)/bis[4-(3-aminophenoxy)-phenyl] sulfone ( <i>m</i> BAPPS)
ODA	oxydianiline
PCL	poly(caprolactonediol)
PDMS	poly(dimethylsiloxane)
PET	poly(ethylene terephthalate)
PMDA	pyromellitic dianhydride
PPG	poly(propyleneglycol)
PPO	poly(propylene oxide)
PTMG	poly(tetramethyleneglycol)
PUI	poly(urethaneimide)
PVC	poly(vinylchloride)
SSE	sum of squares due to error
SSR	sum of squares of regression
SST	total sum of squares
TFE/BDD65	a glassy copolymer containing 65 mol% 2,2-bis (trifluoromethyl)-4,5-difluoro-1,3-dioxole (BDD) and 35 mol% tetrafluoroethylene
TFE/BDD87	a glassy copolymer containing 87 mol% 2,2-bis (trifluoromethyl)-4,5-difluoro-1,3-dioxole (BDD)

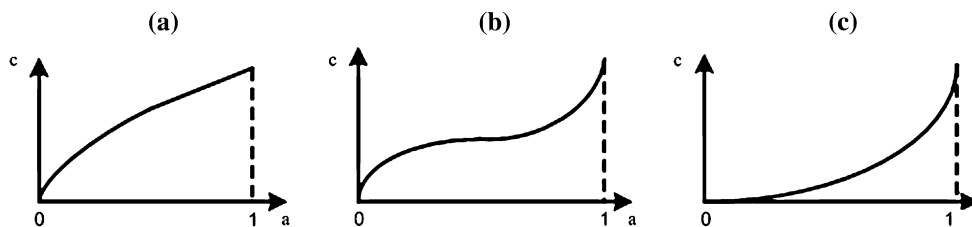


Fig. 1. Vapor sorption isotherms in glassy polymers.

Conventional dual mode sorption (CDMS) model is known to be quite effective in describing Type 1 sorption isotherms of gas or vapor in the glassy polymers [12–18]. It assumes that penetrant molecules are partitioned into two distinct populations, which are in dynamic equilibrium with each other: (i) penetrant molecules sorbed by a dissolution mechanism in the equilibrium dense polymer matrix (Henry's law population—just like gas sorption in rubbery polymers) and (ii) penetrant molecules filling the non-equilibrium unrelaxed, molecular-scale gaps (microvoids) frozen into the glassy state (Langmuir population), as shown in Fig. 2. However, this model cannot describe Types 2 and 3 sorption isotherms effectively.

Engaged species induced clustering (ENSIC) model has been approved to be highly successful in modeling Type 3 vapor sorption isotherms and is better than the conventional Flory–Huggins and related models [19,20]. However, it is unsatisfactory in modeling Type 2 sorption isotherms.

Despite having appeared in an article as early as 1946, the Guggenheim–Anderson–de Boer (GAB) model has agreed extremely well with Type 2 isotherms such as vapor especially water vapor sorption data in food and related natural materials quite recently [21–24]. However, the assumption of the GAB model that all the sorption sites are equivalent is inconsistent with the glassy polymers which are considered to have two species of sorption sites as the CDMS model assumes.

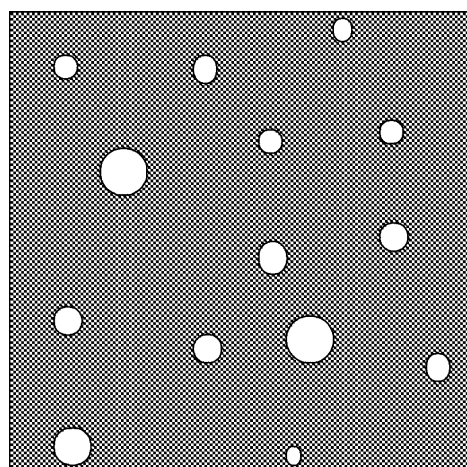


Fig. 2. Schematic of the surface of a glassy polymer.

The objective of present work is to develop a model which can describe all the types of isotherms of vapor sorption in the glassy polymers effectively and reasonably. To this end, based on multilayer sorption theory on which the GAB equation is based, a new dual mode sorption (DMS) model for vapor sorption in the glassy polymers is deduced. One assumption has been made in this model that the vapor sorption in the polymers is composed of two parts, one of which occurs in the equilibrium matrix region of the glassy polymers which is a downward curve similar to that in rubbery polymers, the other happens in the non-equilibrium microvoids which is an upward curve. The mathematical meanings and the physico-chemical significances of the parameters in the new model are analyzed. The new model is proved to agree extremely well with all types of vapor sorption isotherms known in the glassy polymers in the present work.

## 2. Theoretical backgrounds

### 2.1. CDMS and ENSIC models

According to the CDMS model, the penetrant concentration in the glassy polymers is expressed analytically as a sum of two contributions to penetrant sorption [12–18]:

$$c = c_D + c_H \quad (1)$$

$c_D$  and  $c_H$  are given as

$$c_D = k_D p \quad (2)$$

$$c_H = \frac{C'_H b p}{1 + b p} \quad (3)$$

Then,  $c$  becomes

$$c = k_D p + \frac{C'_H b p}{1 + b p} \quad (4)$$

where  $c_D$  and  $c_H$  are the penetrant concentrations by Henry's law mode and Langmuir mode, respectively;  $k_D$  is the Henry's law dissolution constant;  $b$  is the microvoid affinity constant;  $C'_H$  is the Langmuir saturation constant.

For vapor sorption, the original CDMS equation (Eq. (4)) also can be rewritten as

$$c = k_D p_0 \frac{p}{p_0} + \frac{C'_H b p_0 \frac{p}{p_0}}{1 + b p_0 \frac{p}{p_0}} = k_{D0} a + \frac{C'_H b_0 a}{1 + b_0 a} \quad (5)$$

where  $k_{D0} = k_D p_0$ , which is actually penetrant activity coefficient at finite dilution in the matrix region of the glassy polymer;  $b_0 = b p_0$  is the microvoid affinity constant in the form of activity.

Then  $c_D$  and  $c_H$  are expressed as

$$c_D = k_{D0} a \tag{6}$$

$$c_H = \frac{C'_H b_0 a}{1 + b_0 a} \tag{7}$$

The second-order derivative of Eq. (5) with respect to  $a$  is then given as

$$\frac{d^2 c}{da^2} = -\frac{2C'_H b_0^2}{(1 + b_0 a)^3} < 0 \tag{8}$$

This illustrates that the CDMS equation is an upward curve and has no inflection point. Hence, the CDMS model cannot be utilized to describe Type 2 and Type 3 vapor sorption isotherms effectively.

The ENSIC model is, in fact, derived from a rather simple mechanistic approach assuming two elementary sorption processes for a molecule in the vapor phase [19,20]:

- (1) condensation on a polymer site with a probability related to the affinity,  $k_p$ , of a penetrant molecule towards a polymer site; and
- (2) condensation on a previously sorbed penetrant molecule related to the affinity,  $k_s$ , of a penetrant molecule towards a like molecule.

The relationship between the increase of sorbed solvent molecule number  $dn_s$  and the pressure increase in the gaseous phase  $dp$  can be expressed as

$$dn_s = (k_p n_p + k_s n_s) dp \tag{9}$$

where  $n_p$  and  $n_s$  are the polymer segment number and the solvent number in the polymer matrix, respectively.

Integration of Eq. (9) gives the function of the ENSIC model [19]

$$c = \left( \frac{k_p}{k_s - k_p} \right) (\exp((k_s - k_p)a) - 1) \tag{10}$$

If there is no preferential affinity between  $k_p$  and  $k_s$ , i.e.  $k_p = k_s$ , integration of Eq. (9) gives linear relationship between  $c$  and  $a$ , and Henry's dissolution occurs.

The second-order derivative of Eq. (10) with respect to  $a$  is then given as

$$\frac{d^2 c}{da^2} = k_p (k_s - k_p) \exp(k_s - k_p) a \tag{11}$$

$\frac{d^2 c}{da^2} \neq 0$  unless the relationship between  $a$  and  $c$  is linear, i.e.  $k_p = k_s$ . This indicates that the ENSIC equation also has no inflection point. Hence, the ENSIC model cannot be utilized to describe Type 2 vapor sorption isotherms effectively.

Therefore, both the CDMS and ENSIC models are ineffective in modeling sigmoidal isotherms in that there are no inflection points in them.

## 2.2. New dual mode sorption model

### 2.2.1. Statistical multilayer sorption theory GAB model based on

It is well known that the original GAB model can be derived by kinetic as well as by statistical approaches. The present work utilizes the statistical one. Let the sorption system consist of  $X$  sorbate molecules bound to an array of  $N$  sorption sites. The first shell of vapor covers the glassy polymer surface and is tightly bound in a monolayer. Subsequent layers of vapor have weaker interactions with the polymer surface. The interactions between the molecules in these layers and the polymer range in energy level  $s$  somewhere between those of the first layer molecules and the bulk liquid.

For the derivation of the GAB equation, some assumptions are made. The sites are equivalent, distinguishable and independent, and their spatial arrangement is immaterial. On each site, there are  $s$  number of molecules ( $0 \leq s \leq \infty$ ) which can be sorbed in a vertical pile without interactions between molecules sorbed to different sites, i.e. there exists no horizontal interactions. The positions of the molecules in the sorption pile are distinguishable and the thermodynamic state (chemical potential) of the sorbed molecules is regulated by an outer gas phase at a given constant temperature  $T$  and variable pressure  $p$ . Under all these assumptions, the grand partition function,  $\Xi$ , of the system is related to the partition function,  $Q$ , of each site as

$$\Xi(N, T, \mu) = Q(T, \mu)^N \tag{12}$$

and  $Q$  is given as

$$Q = 1 + j_1 \lambda + j_1 j_2 \lambda^2 + j_1 j_2 j_3 \lambda^3 + \dots + j_1 j_2 \dots j_n \lambda^n \tag{13}$$

where  $\mu$  is the chemical potential of the molecules of the sorbed vapor;  $\lambda$  is the corresponding absolute activity, and  $\lambda = \exp(\mu/RT)$ ;  $j_i$  ( $1 \leq i \leq n$ ) is the partition function of a molecule in layer  $i$  of the sorption pile. Then the average number,  $\bar{X}$ , of molecules on the sorbed sites in the polymer is expressed as

$$\bar{X} = kT \left( \frac{\partial \ln \Xi}{\partial \mu} \right)_{N,T} = \lambda \left( \frac{\partial \ln \Xi}{\partial \lambda} \right)_{N,T} = N \lambda \left( \frac{\partial \ln Q}{\partial \lambda} \right)_T \tag{14}$$

The average number,  $s$ , of the molecules per site is given as

$$s = \bar{X}/N = \lambda \left( \frac{\partial \ln Q}{\partial \lambda} \right)_T = \frac{j_1 \lambda + 2j_1 j_2 \lambda^2 + 3j_1 j_2 j_3 \lambda^3 + \dots + n j_1 j_2 \dots j_n \lambda^n}{1 + j_1 \lambda + j_1 j_2 \lambda^2 + j_1 j_2 j_3 \lambda^3 + \dots + j_1 j_2 \dots j_n \lambda^n} \tag{15}$$

$j_i$  can be calculated as

$$j_1 = A_j = A_k j_0 \quad (16)$$

$$j_2 = j_3 = \dots = j_n = k j_0 \quad (17)$$

where  $j_0$  is the partition function of the sorbed molecules in the pure liquid state.

The parameter  $k$  is defined as the ratio of the partition function of molecules sorbed in the multilayer to that of molecules in bulk liquid. It is called correction factor, since it corrects the properties of the multilayer molecules relative to the bulk liquid or indicates the difference between the liquid molecules and multilayer molecules. Parameter  $A$  is defined as the ratio of the partition function of the first molecule sorbed on a site to that of molecules sorbed beyond the first molecule in the multilayer. It is a measure of the strength of binding of sorbed molecules to the primary binding sites. Larger the  $A$ , stronger the sorbed molecules bound in the monolayer and larger the difference between the monolayer molecules and multilayer molecules.  $n$  is the number of sorbed layers.

Then, Eq. (15) becomes

$$s = \frac{c f j_0 \lambda (1 + 2j_n \lambda + 3(j_n \lambda)^2 + \dots + n(j_n \lambda)^{n-1})}{1 + c f j_0 \lambda (1 + j_n \lambda + (j_n \lambda)^2 + \dots + (j_n \lambda)^{n-1})}$$

$$= \frac{c f j_0 \lambda \sum_{i=0}^n i (j_n \lambda)^{i-1}}{1 + c f j_0 \lambda \sum_{i=1}^n (j_n \lambda)^{i-1}} \quad (18)$$

Using the summation formulae of finite geometrical progressions,

$$\sum_{i=0}^n i (j_n \lambda)^{i-1} = \frac{(1 - (n+1)(j_n \lambda)^n + n(j_n \lambda)^{n+1})}{(1 - j_n \lambda)^2} \quad (19)$$

and

$$\sum_{i=1}^n (j_n \lambda)^{i-1} = \frac{1 - (j_n \lambda)^n}{1 - j_n \lambda} \quad (20)$$

and identifying

$$j_0 \lambda = a = p/p_0 \quad (21)$$

$$j_n \lambda = ka \quad (22)$$

Eq. (18) becomes

$$s = \frac{Aka(1 - (n+1)(ka)^n + n(ka)^{n+1})}{(1 - ka)(1 - ka + Aka(1 - (ka)^n))} \quad (23)$$

The sorbate concentration in the polymer is then obtained as

$$c = C_p s = \frac{C_p Aka(1 - (n+1)(ka)^n + n(ka)^{n+1})}{(1 - ka)(1 - ka + Aka(1 - (ka)^n))} \quad (24)$$

where  $C_p$  is the monolayer sorption capacity, which is the vapor content in the polymer corresponding to each sorption site occupied by one vapor molecule. It mainly depends on the

number of sorption sites of the polymer and the properties of sorbed molecules.

If  $n$  is large enough, Eq. (24) simplified as

$$c = \frac{C_p Aka}{(1 - ka)(1 - ka + Aka)} \quad (25)$$

This is the famous GAB equation.

In the kinetic approach, parameter  $A$  measures the difference between molecules in the monolayer and in the multilayer, while parameter  $k$  measures the difference between molecules in the multilayer and in the bulk liquid.  $k$  and  $A$  are calculated as

$$k = k_0 \exp\left(\frac{H_L - H_n}{RT}\right) \quad (26)$$

$$A = A_0 \exp\left(\frac{H_m - H_n}{RT}\right) \quad (27)$$

where  $k_0$  and  $A_0$  are pre-exponential factors;  $H_L$  is the heat of condensation of pure vapor;  $H_m$  and  $H_n$  are the heat of sorption of monolayer and multimolecular layers ( $n$  layers) of the vapor, respectively.

Since the multilayer molecules are less firmly bound than the bulk liquid molecules,  $k$  will be less than unity.

There are three special cases for the multilayer sorption isotherms.

If  $n = 1$ , i.e. it is a monolayer sorption, Eq. (25) is simplified as

$$c = \frac{C_p Aka}{1 + Aka} \quad (28)$$

This equation is just like Langmuir adsorption equation.

If the first layer molecules have the same partition functions as those of the other layers or the first layer molecules have the same heat of sorption as those in other layers, i.e.  $A = 1$ , and  $n$  is large enough, Eq. (24) or (25) is simplified as

$$c = \frac{C_p ka}{1 - ka} \quad (29)$$

If the layers other than the first layer have the same partition functions as those of the pure liquid, i.e.  $k = 1$ , Eq. (25) becomes

$$c = \frac{C_p Aa}{(1 - a)(1 - a + Aa)} \quad (30)$$

This is the famous Brunauer, Emmett and Teller (BET) equation.

### 2.2.2. New dual mode sorption model

Four assumptions are made for the new dual mode sorption model:

- (1) The sorption sites in a glassy polymer material can be divided into two different species; one is located in the matrix region of the polymer and the other in the microvoids.

- (2) All the molecules in the matrix region of the polymer have the same partition functions.
- (3) It is GAB sorption in the microvoid region of the polymer.
- (4) The molecules in the layers other than the first in the microvoid region have the same partition function as those in the matrix region.

According to the second assumption, sorption in the matrix region as follows:

$$c_1 = C_{p1}s_1 = \frac{C_{p1}k_1a}{1 - k_1a} \quad (31)$$

$C_{p1}$  is the monolayer sorption capacity in the matrix region of the polymer, which is interpreted as the vapor content corresponding to each sorption site occupied by one vapor molecule in this region.  $k_1$  measures the difference between molecules in the multilayer and in the bulk liquid in the matrix region of the polymer.

This assumption is suitable for vapor molecules diffusing through the polymer both individually and in clusters.

Fig. 3 illustrates vapor molecules diffusing through the polymer individually.  $n$  vapor molecules sequentially sorb on the surface of the polymer and then diffuse through the polymer, as shown in Fig. 3(a). Then all the vapor molecules will have the same partition functions or have the same heat of sorption in this case. It is equivalent to that the  $n$  molecules which are sorbed in a vertical pile have the same partition function as that of the first molecule in the matrix region of the polymer, as shown in Fig. 3(b).

Fig. 4 illustrates sorption in the matrix region of a polymer for vapor molecules which diffuse through the polymer in clusters. Provided that three molecules are in a cluster, they sorb on the surface of the polymer, as shown in Fig. 4(a).

Then each of the molecules will have the same partition function. This is equivalent to that the three molecules which are sorbed in a vertical pile have the same partition functions as that of the first molecule in the matrix region of the polymer, as shown in Fig. 4(b).

Of course, if  $m$  clusters sequentially sorb on the surface of the polymer and then diffuse through the polymer, the assumption holds and the sorption follows  $c_1 = C_{p1}s_1 = \frac{C_{p1}k_1a}{1 - k_1a}$ .

In terms of the third assumption, sorption in the microvoid region as follows:

$$c_2 = \frac{C_{p2}Ak_2a}{(1 - k_2a)(1 - k_2a + Ak_2a)} = C_{p2} \left( \frac{1}{1 - k_2a} + \frac{(A - 1)k_2a}{1 + (A - 1)k_2a} \right) \quad (32)$$

$C_{p2}$  is the monolayer sorption capacity in the microvoid region of the polymer.  $k_2$  measures the difference between molecules in the multilayer and in the bulk liquid in the microvoid region of the polymer.  $A$  measures the difference between molecules in the monolayer and in the multilayer in the microvoid region.

The sorption in this region is essentially divided into two kinds: one is just like the sorption in the matrix region, which follows  $c_{2-1} = C_{p2} \frac{1}{1 - k_2a}$ ; the other is totally dependent on the microvoids, which follows  $c_{2-2} = C_{p2} \frac{(A-1)k_2a}{1 + (A-1)k_2a}$ .

On one hand, if  $A = 1$ , which means the first layer molecules have the same partition functions as those of the other layers or the first layer molecules have the same heat of sorption as those in other layers in the microvoid region, only one mode of sorption occurs on the surface of the polymer. In addition, if  $A = 1$ ,  $c_{2-2} = 0$ , which means the sorption which is totally dependent on the microvoids disappears. The polymer should be in its rubbery state. On the other hand, if a polymer

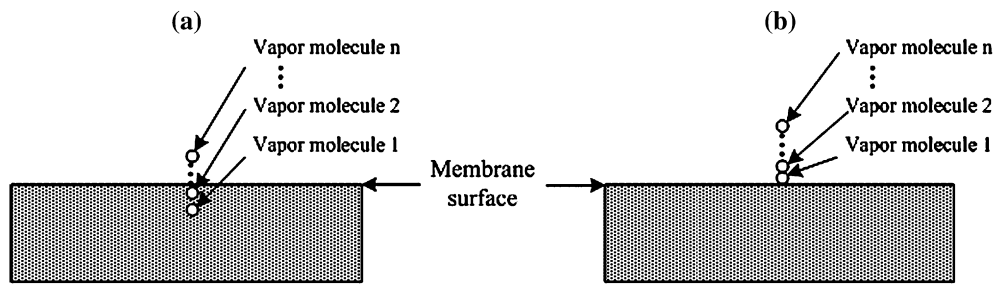


Fig. 3. Schematic of sorption in the matrix region of a polymer for vapor molecules which diffuse through the polymer individually.

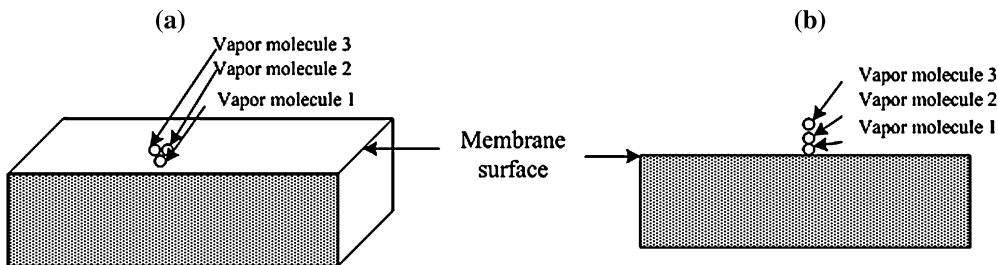


Fig. 4. Schematic of sorption in the matrix region of a polymer for vapor molecules which diffuse through the polymer in clusters.

is in its rubbery state, microvoids in the polymer disappear. Then,  $c_{2-2} = 0$ , and  $A = 1$  accordingly.

According to the third assumption, the following equation is obtained.

$$k_1 = k_2 = k \tag{33}$$

In terms of the first assumption, the sorbate concentration in the polymer is given as

$$c = c_1 + c_2 = C_{p1}s_1 + C_{p2}s_2 = C_{p1}\frac{ka}{1-ka} + C_{p2}\left(\frac{ka}{1-ka} + \frac{(A-1)ka}{1+(A-1)ka}\right) \tag{34}$$

It is a four-parameter equation.

Since the surface area of the matrix region is much greater than that of microvoid region, the following inequality holds.

$$C_{p1}\frac{ka}{1-ka} \ll C_{p2}\frac{ka}{1-ka} \tag{35}$$

Then Eq. (34) becomes

$$c = C_{p1}\frac{ka}{1-ka} + C_{p2}\frac{(A-1)ka}{1+(A-1)ka} \tag{36}$$

Since both  $C_{p1}$  and  $C_{p2}$  are mainly dependent on the properties of the polymer and the vapor, let

$$c = C'_p(s_1 + s_2) \tag{37}$$

Then,

$$C'_p = C_{p1}\frac{s_1}{s_1 + s_2} + C_{p2}\frac{s_2}{s_1 + s_2} \tag{38}$$

$C'_p$  is the weighted mean value of the sorption capacity of the polymer to the sorbate.

Since  $s_1$  and  $s_2$  are functions of  $a$ ,  $C'_p$  is not a constant over the entire range of activity.

Let

$$\bar{s}_1 = \frac{\int_0^1 s_1 da}{1-0} = \int_0^1 s_1 da \tag{39}$$

$$\bar{s}_2 = \frac{\int_0^1 s_2 da}{1-0} = \int_0^1 s_2 da \tag{40}$$

where  $\bar{s}_1$  and  $\bar{s}_2$  are the average values of the average number of sorbed molecules per site in the matrix region and microvoids of the polymer over the entire range of activity, respectively.

Let

$$\bar{C}_p = C_{p1}\frac{\bar{s}_1}{\bar{s}_1 + \bar{s}_2} + C_{p2}\frac{\bar{s}_2}{\bar{s}_1 + \bar{s}_2} \tag{41}$$

$\bar{C}_p$  is the weighted mean value of the sorption capacity of the polymer to the sorbate based on  $\bar{s}_1$  and  $\bar{s}_2$ . It is a constant at a given temperature. If  $\bar{s}_2 = \bar{s}_1$ , the sorption site in the microvoid region is equivalent to that in the matrix region. Otherwise, they are different. For example, if  $\bar{s}_2 = 2\bar{s}_1$ , one sorption site in the microvoid region is equivalent to two sites in the matrix region.

Then,  $c_1$  and  $c_2$  become

$$c_1 = \bar{C}_p s'_1 = \bar{C}_p \frac{k'a}{1-k'a} \tag{42}$$

$$c_2 = \bar{C}_p s'_2 = \bar{C}_p \frac{(A'-1)k'a}{1+(A'-1)k'a} \tag{43}$$

where  $s'_1$  and  $s'_2$  are the average values of the average number of sorbed molecules per site in the matrix region and microvoids of the polymer based on  $\bar{C}_p$ , respectively;  $k'$  is the ratio of the partition function of molecules sorbed in the multilayer to that of molecules in bulk liquid based on  $\bar{C}_p$ ;  $A'$  is the ratio of the partition function of the first molecule sorbed on a site to that of molecules sorbed beyond the first molecule in the multilayer based on  $\bar{C}_p$ .

The sorbate concentration in the polymer is given as

$$c = \bar{C}_p \frac{k'a}{1-k'a} + \bar{C}_p \frac{(A'-1)k'a}{1+(A'-1)k'a} \tag{44}$$

This is the new DMS equation which has three parameters. Therefore, in terms of Eq. (44), the new DMS model for vapor sorption in glassy polymers can be explained as follows. The sorption is contributed to two modes, as shown in Fig. 5, one of which occurs in the matrix region of the glassy polymers and follows  $c_1 = \bar{C}_p \frac{k'a}{1-k'a}$  which is a downward curve similar to that in rubbery polymers; the other happens in the microvoids and follows  $c_2 = \bar{C}_p \frac{(A'-1)k'a}{1+(A'-1)k'a}$  which is an upward curve. The total sorption amount of vapor molecules in the glassy polymers is equal to the sum of the two species.

As stated before,  $\bar{C}_p$  is the weighted mean value of the sorption capacity of a polymer to a vapor. It mainly depends on the structure and the state of the polymer. Besides, the size of the vapor molecule also has some influence on the sorption capacity. For example, there are three sorption sites for larger vapor A molecules, and eight for smaller vapor B molecules, as illustrated in Fig. 6.

According to both the statistical and kinetic approaches,  $k'$  is the difference between the interaction of vapor molecules (shown in Fig. 7(a)) and that of the vapor molecule and a polymer molecule segment (shown in Fig. 7(b)). It is essentially an indication of the interaction between the vapor molecule and the polymer molecule segment. Larger  $k'$  indicates stronger interaction between the vapor and the polymer.

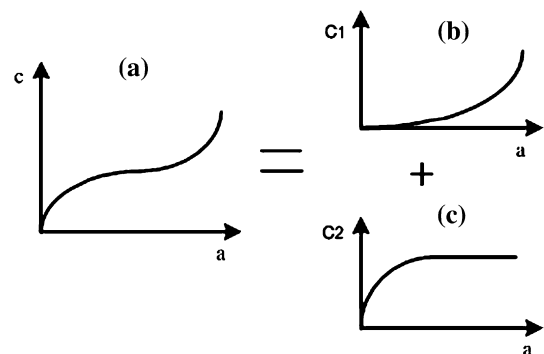


Fig. 5. Schematic representation of the new DMS model.

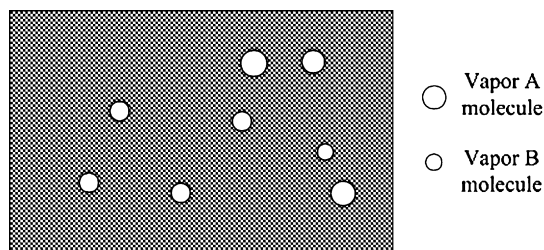


Fig. 6. Influences of the sizes of the vapor molecules on the sorption capacity.

The mathematical meaning of  $k'$  is to demonstrate the magnitude and the curvature of  $c_1$ , as illustrated in Fig. 8. Larger the value of  $k'$ , stronger the interaction between polymer and vapor, greater the departure from linearity, and more the sorbed vapor molecules in the polymer, and vice versa. For example, water vapor/hydrophilic polymer systems have higher values of  $k'$ , while water vapor/hydrophobic polymer systems have lower values of  $k'$ .

As analyzed before,  $A'$  is the difference between the interaction of a microvoid and the first molecule sorbed on it and those of the microvoid and the molecules sorbed beyond the first molecule in the multilayer. In terms of the assumptions of the new model, the interactions of the microvoid and the molecules sorbed beyond the first molecule are equal to those of the molecules and the polymer molecule segments, as shown in Fig. 9(a). Therefore,  $A'$  is actually a measure of the interaction of the vapor molecule and the microvoid (shown in Fig. 9(b)).

Moreover, according to Eq. (43),  $(A' - 1)k'$  measures the affinity between the vapor and the microvoid of the polymer. Since the interaction between the vapor and a polymer in the matrix region and that in the microvoid region share the same  $k'$ , the microvoid properties should be demonstrated only by  $A'$ .

Eq. (43) has a similar form to the Langmuir sorption isotherm Eq. (7). However, for rubbery polymers,  $C_H = 0$  and

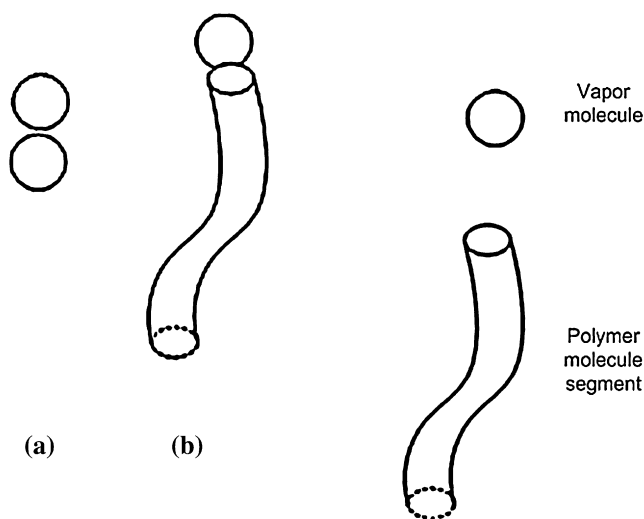


Fig. 7. Schematic of the interaction between vapor molecules (a) and between of the vapor molecule and a polymer molecule segment (b).

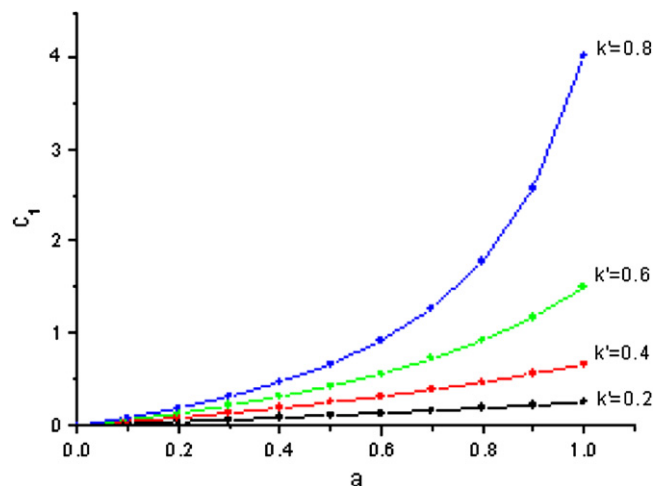


Fig. 8. Schematic of influences of parameter  $k'$  on  $c_1$ .

$b_0 \neq 0$  for Eq. (7), while  $A' = 1$ ,  $\bar{C}_p \neq 0$  for Eq. (43) or (44). Therefore, Eq. (43) is not a strictly Langmuir adsorption.

Eq. (44) has a similar form to the original GAB equation. However, the GAB equation is used to describe multilayer sorption while Eq. (44) is utilized to describe the vapor/glassy polymer systems as dual mode sorption. The GAB equation assumes that all the sorption sites are equivalent while there are two different species of sorption sites in the new DMS model.

The relationship between the CDMS model and the new model is analyzed as follows.

If  $k' \ll 1$ , Eq. (42) becomes

$$c_1 = \bar{C}_p k' a \tag{45}$$

Eq. (44) then changes to

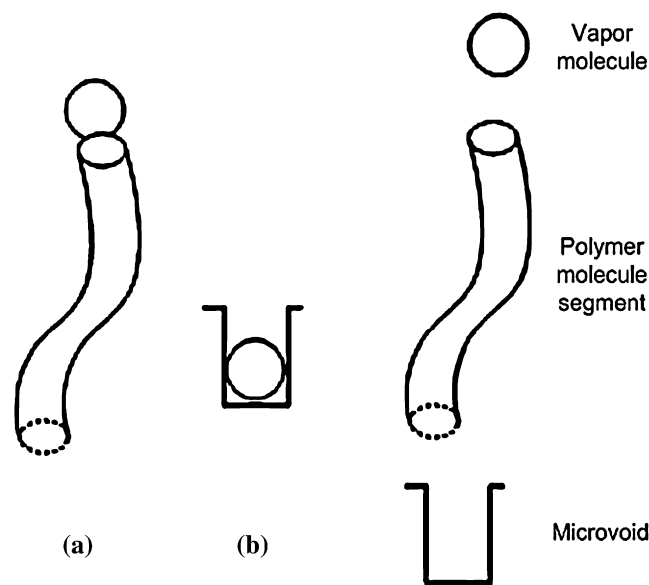


Fig. 9. Schematic of the interaction between the vapor molecule and a polymer molecule segment (a) and that between the vapor molecule and a microvoid of the polymer (b).



$$c = \bar{C}_p k' a + \bar{C}_p \frac{(A' - 1)k' a}{1 + (A' - 1)k' a} \quad (46)$$

Let  $k_1 = C_p k'$ , and  $b' = (A' - 1)k'$ , Eq. (46) becomes

$$c = k_1 a + \bar{C}_p \frac{b' a}{1 + b' a} \quad (47)$$

It has the same form as the CDMS model (Eq. (4)). Therefore, the CDMS model can be considered to be a special case of the new DMS model.

If  $A' = 1$ ,  $c = c_1$  in terms of Eq. (44), indicating that the microvoids in the polymers disappear and the polymers are in their rubbery states. Therefore, a rubbery polymer can be also considered to be a special case of the new model.

The second-order derivative of Eq. (42) with respect to  $a$  is then given as

$$\frac{d^2 c_1}{da^2} = \frac{2\bar{C}_p k'^2}{(1 - k'a)^3} > 0 \quad (48)$$

Hence, Eq. (42) is strictly convex, that is, vapor isotherm in the equilibrium matrix region of the polymer is strictly convex over the entire region of activities.

The second-order derivative of Eq. (43) with respect to  $a$  is then given as

$$\frac{d^2 c_2}{da^2} = -\frac{2\bar{C}_p b'^2}{(1 + b'a)^3} \leq 0 \quad (49)$$

Eq. (43) is concave, meaning that the vapor isotherm in the non-equilibrium microvoids of the polymer is concave over the entire region of activities.

Therefore, Eqs. (42) and (43) have opposite convexities.

The new DMS model can be utilized to describe all the three types of vapor sorption isotherms, shown in Fig. 1, in the glassy polymers.

### 2.3. Theory and derivation of curve fitting

Nonlinear (multiparameter) regressions of experimental data have been performed using a common algorithm based on the Newton–Raphson method. Two parameters, the sum of squares due to error (SSE) and  $R^2$  are utilized to estimate the goodness of fit statistics for parametric models [25]. SSE measures the total deviation of the predicted values from the experiment values, which is also called the summed square of residuals, i.e.

$$SSE = \sum_{i=1}^n (y_i - \hat{y}_i)^2 \quad (50)$$

where  $y_i$ ,  $\hat{y}_i$  are the experiment value and predicted value, respectively.

$R^2$  is the square of the correlation between the response values and the predicted response values, which is defined as the ratio of the sum of squares of the regression (SSR) and the total sum of squares (SST), i.e.

$$R^2 = \frac{SSR}{SST} \quad (51)$$

and SSR is defined as

$$SSR = \sum_{i=1}^n (\hat{y}_i - \bar{y}_i)^2 \quad (52)$$

SST is

$$SST = \sum_{i=1}^n (y_i - \bar{y}_i)^2 \quad (53)$$

where  $\bar{y}_i$  is the mean value.

## 3. Results and discussion

### 3.1. Verification of the new DMS model

It is extremely difficult to verify experimentally the dual mode sorption models directly, whether it is the conventional or the new, in that it is almost impossible to measure vapor concentrations in the polymer matrix and in the microvoid region separately. However, the experiment data can be obtained for a special case,  $A' = 1$  which indicates that the microvoids in the polymer disappear and the polymer should be in its rubbery state. In addition, if the assumptions of the new DMS model for vapor sorption in polymers are valid,  $c_1 = \bar{C}_p \frac{k'a}{1 - k'a}$  can fit the experiment data well. On the other hand, if a polymer is in its rubbery state,  $A'$  should be equal to 1 when the vapor sorption in the polymer is modeled by the new DMS equation. Moreover,  $A' \neq 0$  for vapor sorption in a polymer with Type 3 isotherm indicates that the polymer is glassy.

#### 3.1.1. Example 1

Fig. 10 presents isotherms of water vapor sorption in nylon 6,6 at 25 °C (○), 35 °C (△), and 45 °C (▽). The solid lines are derived from the new DMS equation.

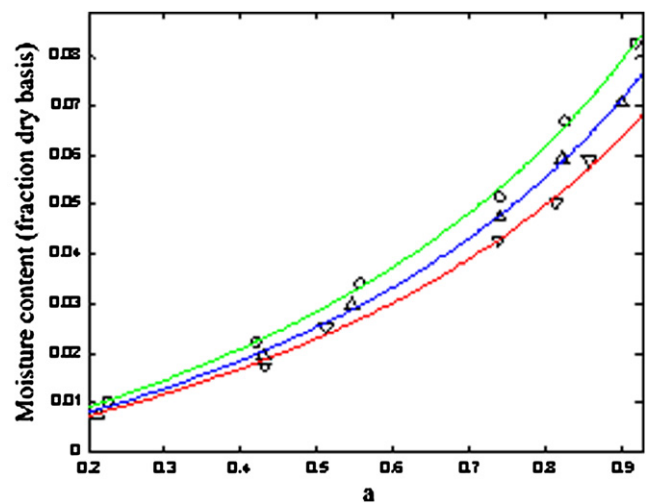


Fig. 10. Water vapor sorption isotherms of nylon 6,6 at 25 °C, 35 °C, and 45 °C respectively. (○) Sorption at 25 °C; (△) sorption at 35 °C; (▽) sorption at 45 °C. The solid lines are derived from the new DMS equation. All the data are from Ref. [26].

Table 1

Estimated values of the parameters and fitting efficiencies of the new DMS model for water vapor sorption isotherms in nylon 6,6 at 25 °C, 35 °C, and 45 °C

Temperature (°C)	$\bar{C}_p$ (fraction dry basis)	$k'$	$A'$	$R^2$
25	0.06317	0.6159	1.02	0.9972
35	0.05574	0.6244	1	0.9992
45	0.05209	0.6121	1	0.9991

The estimated values for the new DMS model parameters are listed in Table 1.

Since the glass transition temperature ( $T_g$ ) of nylon 6,6 is 45 °C, the nylon should be in its glassy state at 25 °C and 35 °C. However,  $A' = 1$  for the sorption isotherms at 35 °C and 45 °C, suggesting the polymer is in rubbery state for such cases.

The polymer is indeed in the rubbery state. This is due to the fact that the sorbed water acted as an effective plasticizer in depressing the glass transition temperature ( $T_g$ ) of the polymer and it has great influence on  $T_g$ . Loong et al. [26] measured  $T_g$  of nylon 6,6 at various water contents using differential scanning calorimetry. The results are presented in Fig. 11.  $T_g = 25.7$  °C at  $a = 0.2$ . Therefore, the nylon 6,6 film at 35 °C and 45 °C actually at its rubbery state.  $A'$  is slightly greater than 1 at 25 °C. This may be due to measurement or fitting errors or due to the fact that there are still a few microvoids in the polymer at 25 °C which is much closer to  $T_g$ .

This case illustrates that if  $A' = 1$ , the polymer is in its rubbery state. Furthermore, both Fig. 10 and Table 1 suggest that the new DMS model describes the experiment data quite satisfactorily. All of these validate the assumptions of the new DMS model.

### 3.1.2. Example 2

Fig. 12 gives sorption isotherms of ethanol vapor in three polymers (polyurethaneimide (PUI) block copolymers), compositions of which are shown in Table 2. Table 3 shows the

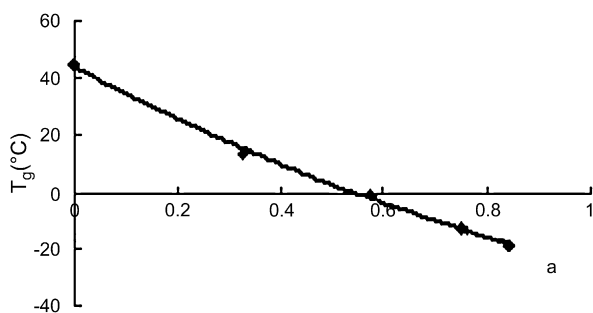


Fig. 11. Glass transition temperature  $T_g$  of nylon 6,6 film as related to moisture content.

Table 2

Chemical compositions of the three PUI copolymers

Abbreviation	Soft segment precursors	$M_n$	Hard block
PTMG650–MDI–AP	Polytetramethyleneglycol	650	Macrodiisocyanate/pyromellitic anhydride (MDI/AP); pyromellitimideurethane
PPG725–MDI–AP	Polypropyleneglycol	725	
PCL1250–MDI–AP	Polycaprolactonediol	1250	

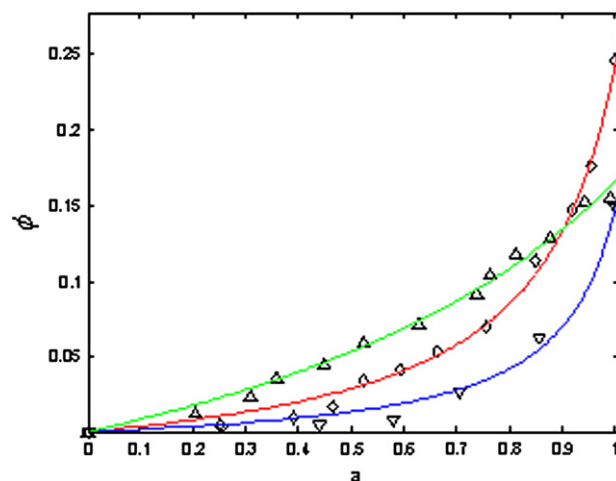


Fig. 12. Sorption of ethanol in three polar elastomers at 30 °C. ( $\Delta$ ) Ethanol sorption in PTMG650–MDI–AP; ( $\diamond$ ) ethanol sorption in PPG725–MDI–AP; ( $\nabla$ ) ethanol sorption in PCL1250–MDI–AP. All of them are the experiment data from Ref. [27]. The solid lines are the results of the sorption isotherms fitted by the new DMS model.

estimated values of the parameters and fitting efficiencies of the new DMS model for ethanol vapor sorption in the three PUI block copolymers. Since the three polymers are rubbery, parameter  $A'$  should be 1 if the new DMS model is valid. Table 3 clearly shows that all the parameters  $A'$ 's of the isotherms are equal to 1. Besides, the new DMS model fits the experiment data well. This example illustrates the rationality of the new DMS model.

### 3.1.3. Other examples

The same conclusions also can be reached by other polymer/vapor systems. Table 4 gives estimated values of the parameters of the new DMS model for five rubbery polymer/vapor systems. Experiment data fitted by the new DMS model were obtained from Kim et al. [28].

Three of the  $A'$  values exactly equal 1. Two of the  $A'$  values are slightly greater than 1, which may result from the measurement or fitting errors. Moreover, according to the square of the correlation,  $R^2$ , between the experiment data and the predicted values, shown in Table 4, the model fits extremely well with

Table 3

Estimated values of the parameters and fitting efficiencies of the new DMS model for ethanol vapor sorption in three PUI block copolymers

Polymer	$\bar{C}_p$ (volume fraction)	$k'$	$A'$	$R^2$
PCL1250–MDI–AP	0.0162	0.9022	1	0.9957
PPG725–MDI–AP	0.0377	0.8668	1	0.9882
PTMG650–MDI–AP	0.1501	0.5249	1	0.9930

Table 4  
Estimated values of the parameters and fitting efficiencies of the new DMS model for five polymer/vapor systems

Polymer	Vapor	Temperature (°C)	$\bar{C}_p$ (weight fraction)	$k'$	$A'$	$R^2$
Poly(dimethylsiloxane) (PDMS)	<i>n</i> -heptane	30	0.2017	0.7203	1.001	0.9999
PDMS	<i>n</i> -octane	30	0.1805	0.7484	1	0.9996
PDMS	<i>n</i> -nonane	40	0.1934	0.7368	1	0.9955
Poly(propylene oxide) (PPO)	Methanol	30	0.0902	0.8660	1.006	0.9996
PPO	Ethanol	30	0.1359	0.8333	1	0.9970

the experiment data. These results validate the assumptions of the new DMS model.

If the conventional DMS model is used for the rubbery polymer,  $c_H = 0$ ,  $c = c_D = k_{D0}a$  which is linear. It does not agree with the experiment data.

### 3.2. Application of the new DMS model to vapor sorption in glassy polymers

#### 3.2.1. Application of the new DMS model to Type 1 vapor sorption isotherms

Water sorption in two polyimide copolymers is taken as an example of this type. Fig. 13 shows isotherms of water vapor sorption in the two polyimide copolymers, pyromellitic dianhydride-4,4'-diaminophenylsulfone (50 mol%)/4,4'-oxydianiline (50 mol%) (PMDA–50DDS/50ODA), and biphenyl tetracarboxylic dianhydride–50 mol% DDS/50 mol% ODA (BPDA–50DDS/50ODA) at 35 °C. Data for these systems were obtained from Huang et al. [2]. These sorption data are fitted by the new DMS and the CDMS models. Tables 5 and 6 list estimated values of the parameters and the fitting efficiencies of the two models for water vapor in these copolymers at 30 °C.

All the isotherms are concave towards the activity axis over the entire activity range. Inflection points of the two isotherms

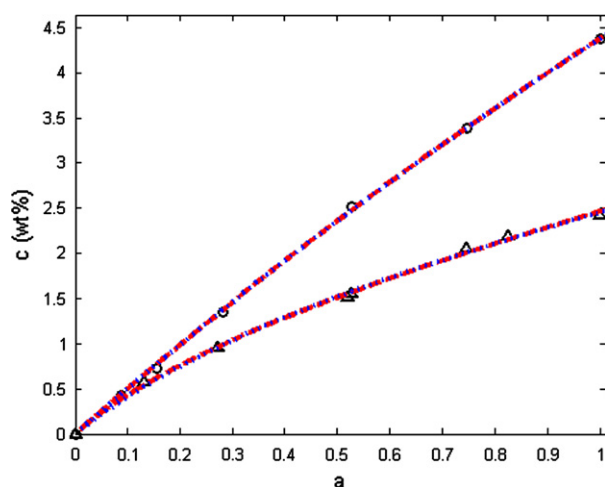


Fig. 13. Water vapor sorption isotherms in two polyimide copolymers, PMDA–50DDS/50ODA and BPDA–50DDS/50ODA at 30 °C. (○) Experiment data for PMDA–50DDS/50ODA; (△) experiment data for BPDA–50DDS/50ODA. The blue dot line and red dash line represent the best fits of the new DMS model and the CDMS model, respectively. Data for these systems were obtained from Huang et al. [2]. (For interpretation of the references to color in this figure legend, the reader is referred to the web version of this article.)

fitted by the new DMS model are at  $a = 20$  and 1.19, respectively, also indicating that all the isotherms are Type 1.

It is well known that this type of vapor sorption data can be accurately described by CDMS model, which is typically used to model gas or vapor sorption in glassy polymers. This example confirms this result. Furthermore, the isotherms obtained by the CDMS and the new DMS models almost coincide with each other, indicating that both of them fit extremely well with the experiment data, as displayed in Fig. 13. Table 6 also suggests that the new DMS model is as effective as the CDMS model in fitting Type 1 vapor sorption isotherms.

Therefore, both the CDMS and the new DMS models describe Type 1 vapor sorption isotherms in glassy polymers extremely well.

#### 3.2.2. Application of the new DMS model to Type 4 vapor sorption isotherms

Since this type of isotherms looks like Type 1, researchers such as Okuno et al. [11] utilized only the CDMS model to fit the experiment data. Present work fits the new DMS and CDMS models to the experiment data referenced from Okuno et al. [11]. Fig. 14 presents water and ethanol vapor sorption isotherms in PVC at 40 °C fitted by the new DMS and CDMS models. Tables 7 and 8 give the estimated values of the parameters and the fitting efficiencies of the two models, respectively.

The inflection points are at  $a = 0.57$  and 0.44, respectively, for water and ethanol vapor sorption in PVC at 40 °C, suggesting that the isotherms are actually Type 2. Both Fig. 14 and

Table 5  
Estimated values of the parameters of the new DMS and the CDMS models for water vapor in dense polyimide copolymers at 30 °C

Polyimide	New DMS model		CDMS model			
	$k'$	$A'$	$\bar{C}_p$ (wt%)	$k_{D0}$ (wt%)	$C'_H$ (wt%)	$b_0$
PMDA–50DDS/50ODA	0.01212	15.85	26.6	0.0009924	30.9	0.1651
BPDA–50DDS/50ODA	0.2091	7.4	2.93	1.473	1.38	2.548

Table 6  
Comparison of the new DMS model with the CDMS model in fitting water vapor in dense polyimide copolymers at 30 °C

Copolymer	Model	SSE	$R^2$
PMDA–50DDS/50ODA	New DMS	3.5E–3	0.9998
	CDMS	3.5E–3	0.9998
BPDA–50DDS/50ODA	New DMS	1.1E–2	0.9979
	CDMS	9.5E–3	0.9981

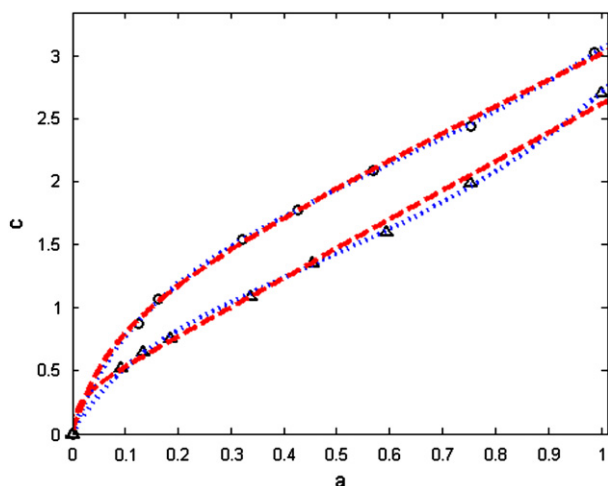


Fig. 14. Sorption isotherms of water and ethanol vapors in PVC at 40 °C. (○) Experiment data for water vapor sorption; (△) experiment data for ethanol vapor sorption; all the data obtained from Okuno et al. [11]. The blue dot line and red dash line represent the best fits of the new DMS model and the CDMS model to the experiment data, respectively. The unit of vertical axis is  $10^{-3}$  g/cm<sup>3</sup> polymer for water vapor sorption and  $10^{-2}$  g/cm<sup>3</sup> polymer for ethanol vapor sorption. Inflection points are at  $a = 0.57$  and  $0.44$  for water vapor and ethanol vapor sorption in the polymer, respectively. (For interpretation of the references to color in this figure legend, the reader is referred to the web version of this article.)

Table 8 indicate that the new DMS model is superior to the CDMS model in fitting Type 4 isotherms.

### 3.2.3. Application of the new DMS model to Type 2 vapor sorption isotherms

Characteristics of water sorption in three glassy copolymers are investigated in this section. The three sulfonated polyimide copolymers were synthesized by copolymerization of 1,4,5,8-naphthalenetetracarboxylic dianhydride (NTDA) and 2,2'-bis(4-aminophenoxy)biphenyl-5,5'-disulfonic acid (*o*BAPBDS) (NTDA-*o*BAPBDS), copolymerization of NTDA and 4,4'-bis(4-aminophenoxy)biphenyl-3,3'-disulfonic acid (BAPBDS) (NTDA-BAPBDS), and copolymerization of NTDA and *o*BAPBDS/bis[4-(3-aminophenoxy)-phenyl] sulfone (*m*BAPPS) (NTDA-*o*BAPBDS/*m*BAPPS(2/1)), respectively.

Water vapor sorption isotherms in the three sulfonated polyimide copolymers at 50 °C fitted by the new DMS model are presented in Fig. 15. The inflection points are at  $a = 0.31$ ,  $0.30$ ,  $0.30$ , respectively, for water sorption in NTDA-*o*BAPBDS, NTDA-BAPBDS and NTDA-*o*BAPBDS/*m*BAPPS(2/1) at 50 °C, suggesting the isotherms are real Type 2.

Tables 9 and 10 give the parameters and the fitting efficiencies of the new DMS for water vapor sorptions in the three sulfonated polyimide copolymers at 50 °C, respectively.

Table 7

Estimated values of the parameters of the new DMS and the CDMS models for sorption isotherms of water and ethanol vapors in PVC at 40 °C

Vapor	New DMS model			CDMS model		
	$k'$	$A'$	$\bar{C}_p$ (g/cm <sup>3</sup> polymer)	$k_{D0}$ (g/cm <sup>3</sup> polymer)	$C'_H$ (g/cm <sup>3</sup> polymer)	$b_0$
Water vapor	0.43	14.14	$1.918E-3$	$22.96E-3$	$3.211E-3$	90.33
Ethanol vapor	0.5633	10.5	$12.73E-3$	$2.01E-3$	$1.094E-3$	12.06

Table 8

Fitting efficiencies of the new DMS and the CDMS models for sorption isotherms of water and ethanol vapors in PVC at 40 °C

Vapor	Model	SSE	$R^2$
Water vapor	New DMS model	$2.09E-9$	0.9997
	CDMS	$6.99E-9$	0.9989
Ethanol vapor	New DMS model	$3.86E-7$	0.9993
	CDMS	$2.24E-6$	0.9959

Both Fig. 15 and Table 10 demonstrate that the new DMS model agrees extremely well with the experiment data for such cases.

Another example of Type 2 isotherm is methanol vapor sorption in cellulose acetate at 25 °C. Sorption data are fitted by three models, new DMS, ENSIC and CDMS, as illustrated in Fig. 16. Estimated values of the parameters of the three models for the sorption are listed in Table 11. Their fitting

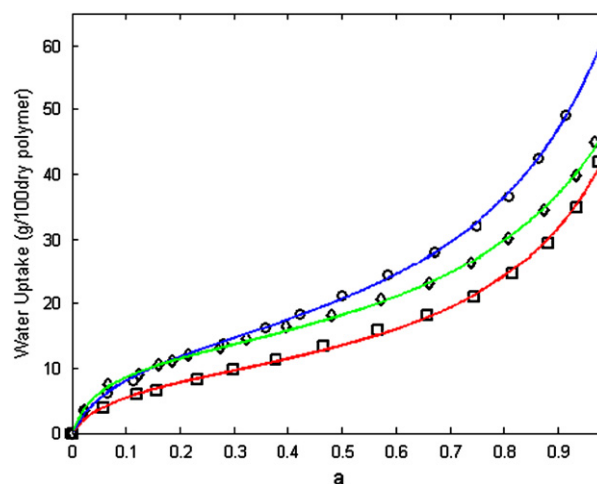


Fig. 15. Water vapor sorption in the three sulfonated polyimide copolymers at 50 °C. (○) Experiment data for sorption in NTDA-*o*BAPBDS; (◇) experiment data for sorption in NTDA-BAPBDS; (□) experiment data for sorption in NTDA-*o*BAPBDS/*m*BAPPS; solid lines represent fit of the new DMS model to the experiment data which were from Ref. [29].

Table 9

Estimated values of the parameters of the new DMS model for water vapor sorption in the three sulfonated polyimide copolymers at 50 °C

Copolymer	New DMS model		
	$k'$	$A'$	$\bar{C}_p$ (g/100 g dry polymer)
NTDA- <i>o</i> BAPBDS	0.7912	12.92	13.97
NTDA-BAPBDS	0.7537	22.57	12.15
NTDA- <i>o</i> BAPBDS/ <i>m</i> BAPPS(2/1)	0.8089	14.42	8.865

Table 10  
Goodness-of-fit evaluations for water vapor sorption in the three sulfonated polyimide copolymers at 50 °C using the new DMS model

Copolymer	SSE	$R^2$
NTDA- <i>o</i> BAPBDS	2.11	0.9993
NTDA-BAPBDS	2.46	0.9991
NTDA- <i>o</i> BAPBDS/ <i>m</i> BAPPS(2/1)	2.96	0.9985

efficiencies are given in Table 12. The inflection point is at  $a = 0.33$ .

Both Fig. 16 and Table 12 illustrated that the new DMS model is obviously superior to the other models, CDMS and ENSIC for this type of sorption.

### 3.2.4. Application of the new DMS model to Type 5 vapor sorption isotherms

Water vapor sorption in cellulose acetate at 25 °C is investigated in this section. Since this type of isotherms look like Type 3, such as water vapor sorption in cellulose acetate at 25 °C, as illustrated in Fig. 17, Perrin et al. [10] utilized the ENSIC model to fit the experiment data. Present work fits the ENSIC, CDMS and new DMS model to the experiment data from Perrin et al. [10].

Fig. 17 displays water vapor sorption isotherms in cellulose acetate at 25 °C fitted by three models, CDMS, ENSIC and new DMS. Tables 13 and 14 give the estimated values of the parameters and the fitting efficiencies of the three models.

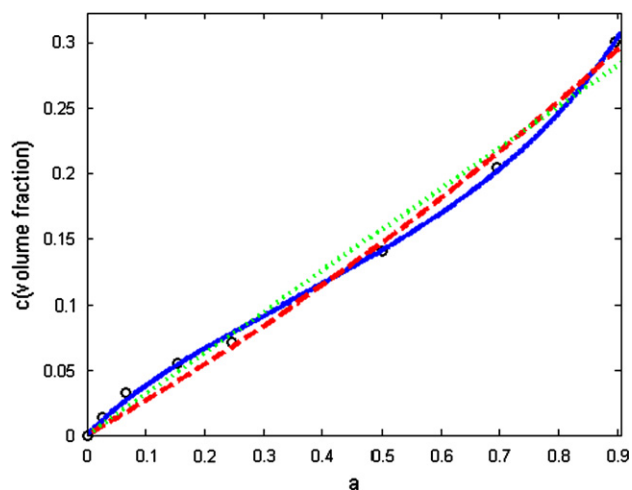


Fig. 16. Sorption isotherms for methanol vapor in cellulose acetate at 25 °C. (○) Experiment data from Perrin et al. [10]. The blue solid line, red dash line and green dot line represent the best fit of the three models, new DMS, ENSIC and CDMS, respectively. (For interpretation of the references to color in this figure legend, the reader is referred to the web version of this article.)

Table 12  
Fitting efficiencies of the three models for methanol vapor sorption in cellulose acetate at 25 °C

Model	SSE	$R^2$
New DMS model	9.94E-5	0.9987
CDMS	1.09E-3	0.9859
ENSIC	6.92E-4	0.9911

Both Fig. 17 and Table 14 clearly illustrated that the new DMS model is obviously superior to the other models, CDMS and ENSIC, for this type of sorption.

### 3.2.5. Application of the new DMS model to Type 3 vapor sorption isotherms

Ethanol vapor sorption in cellulose acetate at 25 °C is investigated in this section. Fig. 18 displays ethanol vapor sorption isotherms in the cellulose acetate at 25 °C fitted by three models, CDMS, ENSIC and new DMS. Tables 15 and 16 give the estimated values of the parameters and the fitting efficiencies of the three models.

Although the sorption isotherm of water vapor is an upward curve, the parameter  $A'$  equals 1.87, indicating that the water sorption in the microvoids of the polymer still exists and the polymer is in its glassy state. Cellulose acetate at 25 °C is in fact in its glassy state. This illustrates that the new DMS model is reasonable.

Both Fig. 18 and Table 16 show that the new DMS model agrees slightly better than the ENSIC model and obviously better than the CDMS model for such case.

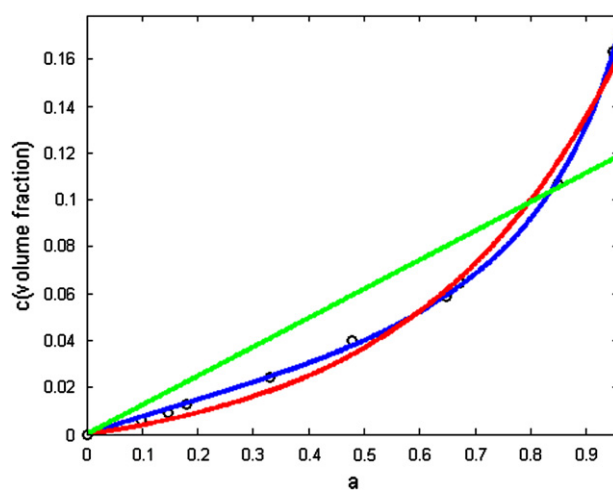


Fig. 17. Water vapor sorption in cellulose acetate at 25 °C. (○) Experiment data from Perrin et al. [10]. The blue, red and green lines represent the best fit of the three models, new DMS, ENSIC and CDMS, respectively. The inflection point is at  $a = 0.14$ . (For interpretation of the references to color in this figure legend, the reader is referred to the web version of this article.)

Table 11

Estimated values of the parameters of the three models, new DMS, CDMS and ENSIC for methanol vapor sorption in cellulose acetate at 25 °C

New DMS model			CDMS model			ENSIC model		
$k'$	$A'$	$\bar{C}_p$ (volume fraction)	$k_{D0}$ (volume fraction)	$C_{H1}$ (volume fraction)	$b_0$	$k_s$	$k_p$	
0.7058	5.24	0.1228	0.3128	0.05381	0.01371	0.2557	0.7848	

Table 13

Estimated values of the parameters of the three models, new DMS, CDMS and ENSIC for water vapor sorption in cellulose acetate at 25 °C

New DMS model			CDMS model		ENSIC model		
$k'$	$A'$	$\bar{C}_p$ (volume fraction)	$k_{D0}$ (volume fraction)	$C'_H$ (volume fraction)	$b_0$	$k_s$	$k_p$
0.845	2.59	0.03532	0.1238	0.006557	0.003025	0.2557	0.7848

Table 14

Fitting efficiencies of the three models for water vapor sorption in cellulose acetate at 25 °C

Model	SSE	$R^2$
New DMS model	1.49E–5	0.9994
CDMS	3.76E–3	0.8469
ENSIC	2.55E–5	0.9896

Table 15

Estimated values of the parameters of the three models, new DMS, CDMS and ENSIC for ethanol vapor sorption in cellulose acetate at 25 °C

New DMS model			CDMS model		ENSIC model		
$k'$	$A'$	$\bar{C}_p$ (volume fraction)	$k_{D0}$ (volume fraction)	$C'_H$ (volume fraction)	$b_0$	$k_s$	$k_p$
0.4729	1.87	0.2125	0.2225	0.05125	0.01732	0.1719	0.86

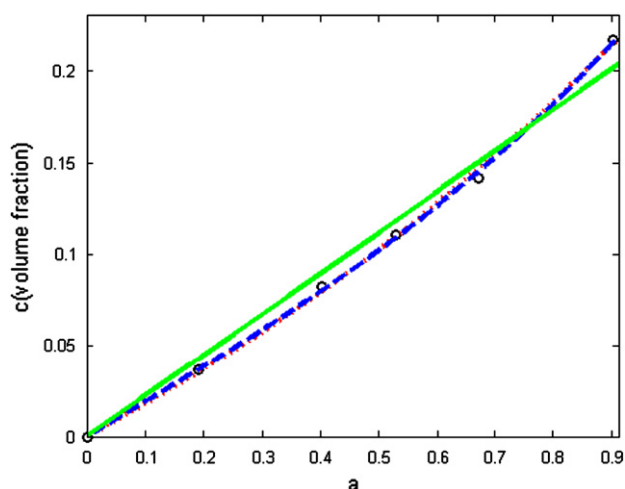


Fig. 18. Ethanol vapor sorption in cellulose acetate at 25 °C. (○) Experiment data from Perrin et al. [10]. The blue dash line, red dot line and green solid line represent the best fit of the three models, new DMS, ENSIC and CDMS, respectively. (For interpretation of the references to color in this figure legend, the reader is referred to the web version of this article.)

Comparisons of the new DMS model with the CDMS and the ENSIC models for all types of vapor sorption isotherms in glassy polymers are summarized in Table 17. The table clearly shows that the new DMS model fits the experiment data extremely well for all types of vapor sorption isotherms in the glassy polymers while the other models can describe only one type of the isotherms very well.

#### 4. Conclusions

1. Like the CDMS model, the new DMS model for vapor sorption in glassy polymers assumes that two species of the sorbed molecules contribute to the penetrant concentration in

Table 16

Comparison among the fitting efficiencies of the three models for ethanol vapor sorption in cellulose acetate at 25 °C

Model	SSE	$R^2$
New DMS model	2.14E–5	0.9993
CDMS	4.58E–4	0.9846
ENSIC	4.20E–5	0.9986

Table 17

Comparison of the new DMS model with the CDMS and the ENSIC models for fitting all types of vapor sorption isotherms in glassy polymers

Model	Type 1	Type 2	Type 3	Type 4	Type 5
New DMS	Very good	Very good	Very good	Very good	Very good
CDMS	Very good	Poor	Poor	OK	Poor
ENSIC	Poor	Poor	Very good	Poor	OK

glassy polymers, one of which occurs in the matrix region of the glassy polymers and follows  $c_1 = \bar{C}_p \frac{k'a}{1-k'a}$  which is a downward curve similar to that in rubbery polymers; the other happens in the microvoids and follows  $c_2 = \bar{C}_p \frac{(A'-1)k'a}{1+(A'-1)k'a}$  which is an upward curve. The total sorption amount of vapor molecules in the glassy polymers is equal to the sum of the two species.

2. The new DMS model is reasonable for vapor sorption in glassy polymers.

3. The new DMS model fits the experiment data extremely well for all types of vapor sorption isotherms in the glassy polymers while the CDMS model can describe only Type 1 isotherms very well and the ENSIC model agrees extremely well with only Type 3 isotherms for they have no inflection points.

#### References

- [1] Serad GE, Freeman BD, Stewart ME, Hill AJ. *Polymer* 2001;42: 6929–43.
- [2] Huang Jingui, Cranford Richard J, Matsuura Takeshi, Roy Christian. *J Appl Polym Sci* 2003;87:2306–17.
- [3] Alentiev AYU, Shantarovich VP, Merkel TC, Bondar VI, Freeman BD, Yampolskii YuP. *Macromolecules* 2002;35:9513–22.
- [4] Huang Jingui, Cranford Richard J, Matsuura Takeshi, Roy Christian. *J Membr Sci* 2004;241:187–96.
- [5] Krykin MA, Zinovieva OM, Zinoviev AB. *J Polym Sci Part B Polym Phys* 1999;37:2314–23.

- [6] Gocho Hiromi, Tanioka Akihiko, Nakajima Toshinari. *J Colloid Interface Sci* 1998;200:155–60.
- [7] Watari Tatsuya, Wang Hongyuan, Kuwahara Katsunari, Tanaka Kazuhiro, Kita Hidetoshi, Okamoto Kenichi. *J Membr Sci* 2003;219:137–47.
- [8] Kamaruddin HD, Koros WJ. *J Polym Sci Part B Polym Phys* 2000;38:2254–67.
- [9] Detallante Virginie, Langevin Dominique, Chappet Corinne, Metayer Michel, Mercierb Regis, Pinl Michel. *Desalination* 2002;148:333–9.
- [10] Perrin Laurent, Nguyen Quang Trong, Sacco Daniel, Lochon Pierre. *Polym Int* 1996;42:9–16.
- [11] Okuno Hiroshi, Renzo Kazuhiko, Uragami Tadashi. *J Membr Sci* 1995;103:31–8.
- [12] Koros WJ, Paul DR. *J Polym Sci Polym Phys Ed* 1976;14:687–702.
- [13] Chiou JS, Paul DR. *J Membr Sci* 1987;32:195.
- [14] Koros WJ, Paul DR. *J Polym Sci Polym Phys Ed* 1978;16:1947–63.
- [15] Koros WJ, Chan AH, Paul DR. *J Membr Sci* 1997;2:165–90.
- [16] Bondar VI, Kamiya Y, Yampolskii YP. *J Polym Sci Part B Polym Phys* 1996;34:369–78.
- [17] Pellegrino J, Radebaugh R. *Macromolecules* 1996;29:4985–91.
- [18] Barbari TA, Koros WJ, Paul DR. *J Polym Sci Polym Phys Ed* 1998;26:729.
- [19] Favre E, Clement R, Nguyen QT, Schactzel P, Neel J. *J Chem Soc Faraday Trans* 1993;89:4339–53.
- [20] Favre E, Nguyen QT, Clement R, Neel J. *J Membr Sci* 1996;117:227–36.
- [21] Timmermann EO. *J Chem Soc Faraday Trans 1* 1989;85(7):1631–45.
- [22] Timmermann EO. *Colloids Surf A* 2003;220:235–60.
- [23] Jonquieres Anne, Fane Anthony. *J Appl Polym Sci* 1998;67:1415–30.
- [24] Timmermann EO, Chirife J, Iglesias HA. *J Food Eng* 2001;48:19–31.
- [25] Curve fitting toolbox user's guide. The Math Works, Inc.
- [26] Loong TL, Britt IJ, Marvin AT. *J Appl Polym Sci* 1999;71:197–206.
- [27] Jonquieres Anne, Perrin Laurent, Arnold Stephanie, Lochon Pierre. *J Membr Sci* 1998;150:125–41.
- [28] Kim Jisoo, Choi Eun-hyun, Yoo Ki-Pung, Lee Chul Soo. *Fluid Phase Equilib* 1999;161:283–93.
- [29] Guo XX, Fang JH, Tanaka Kazuhino, Kita Hidetoshi, Okamoto Kenichi. *J Polym Sci Polym Chem Ed* 2004;42:1432–40.